**TEST PARTICLE MODELS OF IONS IN THE PLUME OF ENCELADUS – INTERPRETATION OF INMS DATA.**
S. Sakai[1], T. E. Cravens[1], N. Omidi[2], and M. E. Perry[3], [1]Department of Physics and Astronomy, University of Kansas, Lawrence, KS 66045 (shotaro@ku.edu), [2]Solana Scientific Inc., Solana Beach, CA 92075, [3]The Johns Hopkins University Applied Physics Laboratory, Laurel, MD 20723.

**Introduction:** Cassini observations discovered a dynamic plume on the south pole of Enceladus in 2005 [e.g., 1] and the plume is regarded as a major source of plasma, neutral gas and dust in E ring [e.g., 2-4]. The plume as observed by the Cassini Neutral Mass Spectrometer (INMS) is composed of $H_2O$ (91%), CO or $N_2$ (3.3%), $CO_2$ (3.1%) and $CH_4$ (1.6%) [5]. The Cassini INMS also detected the ion count rate for m/q (mass per charge) and ions of 18, 19, 36 and 37 amu were observed in the plume [6]. These species are thought to be molecular ions such as $H_2O^+$ (m/q = 18), $H_3O^+$ (19), and cluster ions such as $H_2O^+$-$H_2O$ (36) and $H_3O^+$-$H_2O$ (37). They also showed that the $H_3O^+$ generated by ion-neutral reactions is dominant in the plume.

The energy distribution in the plume was examined by the Cassini Plasma Spectrometer (CAPS). The ion energy was between 10 and 100 eV outside the plume, however, it decreased to a few eV in the plume [7].

We have investigated the charcteristics of water group ions in the vicinity of Enceladus using test particle and Monte Carlo methods including collisional processes such as charge exchange and ion-neutral chemical reaction, and compared them with observations of the INMS and CAPS.

**E03 & E07 Flybys:** The INMS detected the ion species on E03 and E07 flybys (Fig. 1). Fig. 1 shows the Cassini orbits with Enceladus coordinate system superposed on the Omidi's electric field we used as background fields [8], energy spectrogram observed by the CAPS and the count rate of $H_3O^+$ (m/q = 19) observed by the INMS for E03 and E07 flybys.

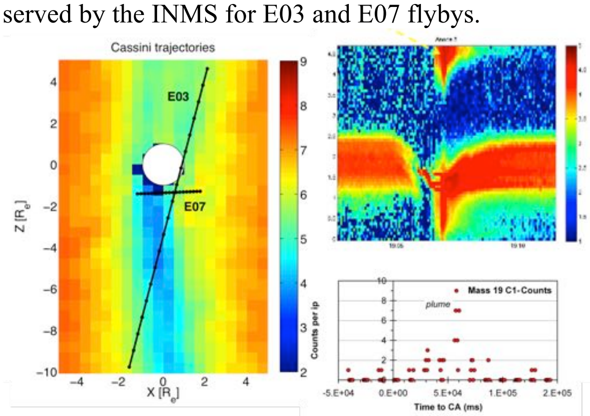


**Figure 1.** Cassini orbits with Enceladus coordinate system superposed on the Omidi's electric field, energy spectrogram by the CAPS and the ion count rate of m/q = 19 by the INMS for E03.

We compare our results with the CAPS and INMS results, and discuss them.

**Model:** We use test particle and Monte Carlo methods to investigate the distribution of water group ions around the Enceladus plume. The number of particles is 1,000,000 and the Enceladus coordinate system is adopted in this model. The positive X is the direction of co-rotation and the positive Y is toward to Saturn with a focus on Enceladus. A box size for simulation is 10 $R_E$ × 10 $R_E$ × 15 $R_E$ (-5 $R_E \le X \le 5$ $R_E$, -5 $R_E \le Y \le 5$ $R_E$ and -10 $R_E \le Z \le 5$ $R_E$) where $R_E$ is the radius of Enceladus (252 km). Particles are set at X = -5 $R_E$ (front model) with the reduced co-rotation speed [9-11]. We calculated energy distribution and ion components with three cases of electric field: (1) the Omidi's electric field, (2) the reduced $E_y$ from Omidi's field which is 25% of the Omidi's $E_y$, and (3) the reduced $E_y$ & $E_z$ from Omdi's field ($E_z$ = -10 μV/m).

*$H_2O^+$-$H_2O$ reactions:* The $H_2O^+$ is given as the initial input of ion since most of $H_3O^+$ which is dominant in the plume are created by $H_2O^+$ [6]. The following $H_2O^+$-$H_2O$ reactions are used:

$$H_2O^+ + H_2O \rightarrow H_2O + H_2O^+$$

$$H_2O^+ + H_2O \rightarrow OH + H_3O^+$$

The cross section for the charge exchange reaction is a constant $10^{-15}$ $cm^{-2}$ and for the chemical reaction depends on the ion energy [12].

*Plume model:* We assume that $H_2O^+$-$H_2O$ reactions only occur in the plume to investigate the ion distribution of the plume. We use one single plume model [13]. The density in the plume $n_{\text{plume}}$ is written by

$$n_{plume}(r,\theta) = n_0\left(\frac{R_E}{r}\right)^2 \exp\left[-\left(\frac{\theta}{H_\theta}\right)^2 - \frac{r-R_E}{H_d}\right]$$

where $n_0$ is the $H_2O$ density at the center of plume on the Enceladus' surface and it is $2.5\times10^9$ $cm^{-3}$, $r$ is the radial distance from the center of Enceladus, $\theta$ is the angular distance from the center of plume, $H_\theta$ the angular width of the plume and it is 12°, and $H_d$ is the depletion length scale and we set it 948 km which equals to four times of the Hill radius [13, 14].

**Energy distribution and species:** Fig. 2 shows the calculated energy-flux distribution for E03. We will also show E07 results. The plume region for E03 is about from 19:07 to 19:08, and for E07 is about from 19:42 to 19:43. The energy distribution of plasma is a few tens to hundreds of eV outside plume in each case. We couldn't find low energy ions for cases (1) and (2) in the plume region. However, ion energy decreased to a few eV (Fig. 2) when the z-component electric field was considered. To obtain the low energy flux, the ion needs to move with ~10 km/s downward (-z direction) because Cassini was almost moving the negative z direction. The gas speed of the neutral plume is

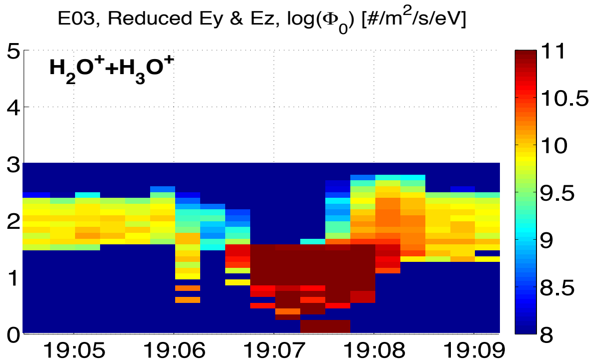


**Figure 2.** Calculated ion flux per energy for E03 with reduced $E_y$ & $E_z$.

about 400 m/s. Therefore, another mechanism was needed to explain the fast downward velocity of ion. We focused on the z component of electric field and could obtain the low energy ion by reducing this field. The cause of the reduced $E_z$ could be dust effect, the density gradient of electron or the Enceladus charging. On the other hand, we were able to obtain low energy ions for E07 in all cases (not shown here). The dominant ion species was $H_3O^+$. This is consistent with INMS observations [6].

**Chemical reaction vs. Photoionization:** We examine what ions are dominant in the plume by using two models: (1) ions generated by only photoionization in the plume (photo-plume model) and (2) ions from the magnetosphere.

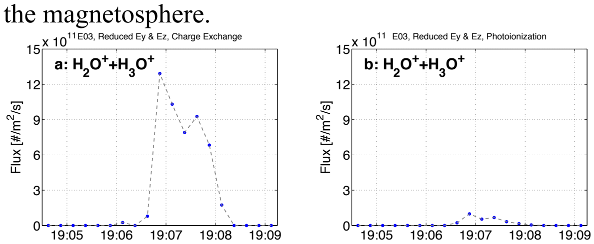


**Figure 3.** Calculated ion total flux for E03 in front model (a) and photo-plume model (b) with reduced $E_y$ & $E_z$.

Fig. 3 shows the calculated total ion flux with reduced $E_y$ & $E_z$ case for E03 orbit. The total flux of front model (panel a) is a order of magnitude larger than that of photo-plume model (panel b). The plume ion is dominated by the magnetospheric ion which is originally generated from the plume gas.

**Interpretation of INMS data:** We compare our results with INMS observations for E03 and E07 flybys. Fig. 4 shows the calculated ion flux per 1 eV with reduced $E_y$ & $E_z$ case for E03 and E07 flybys. The ion velocity vector was confined within 10 degree respect

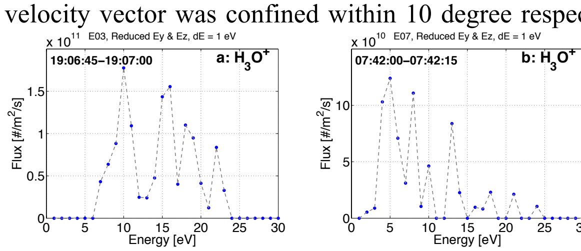


**Figure 4.** Calculated ion flux per 1 eV for E03 (a) and E07 (b) with reduced $E_y$ & $E_z$. The INMS has a field-of-view for ions of ~5 degree.

to the space craft direction for obtaining flux since the INMS has a field of view for ions of ~5 degree. Only energies less than 30 eV were detected within 10 degree. The energy range for E03 is somewhat larger than that for E07 because the s/c velocity of E03 is faster than velocity of E07. The INMS would observe around 20 eV for E03 and 6 eV for E07 because a center of a field of view is about 20 eV for E03 and about 5.6 eV for E07. We will translate the fluxes to count rates and compare with INMS results.

**Summary:** We investigated the energy distribution and the total flux of water group ions around the Enceladus plume. Charge exchange and chemical reactions are considered in this model. Our main results are that: (1) low energy ions were found in the plume when the negative z-component electric field was taken into account, and the dust and density gradient of electron can generate a polarization electric field in the plume, (2) the dominat ion in the plume is $H_3O^+$ generated by a chemical reaction, and (3) photoionization is not effective for the generation of ions in the plume.

**References:** [1] Porco C. C. et al. (2006) *Science, 311,* 1393–1401. [2] Johnson R. E. et al. (2006) *Ap. J., 644,* L137-L139. [3] Jurac S. and Richarson J. D. (2005) *JGR, 110,* A09220. [4] Kivelson M. (2006) *Science, 311,* 1391-1392. [5] Waite J. H. Jr. et al. (2006) *Science, 311,* 1409-1412. [6] Cravens T. E. et al. (2009) *GRL, 36,* L08106. [7] Tokar R. J. et al. (2009) *GRL, 36,* L20105. [8] Omidi N. et al. (2010) *JGR, 115,* A05212. [9] Holmberg M. K. G. et al. (2012) *PSS, 73,* 151-160. [10] Thomsen M. F. et al. (2010) *JGR, 115,* A10220. [11] Sakai S. et al. (2013) *PSS, 75,* 11-16. [12] Lishawa C. R. et al. (1990) *JCP, 93,* 3196-3206. [13] Saur J. et al. (2008) *GRL, 35,* L20105. [14] Fleshman B. L. et al. (2012) *JGR, 117,* E05007.